RSC Advances

ROYAL SOCIETY OF CHEMISTRY

PAPER

View Article Online
View Journal | View Issue

Cite this: *RSC Adv.*, 2022, **12**, 2549

NosZ gene cloning, reduction performance and structure of *Pseudomonas citronellolis* WXP-4 nitrous oxide reductase†

Liyong Hu,[a] Xiaoping Wang,[a] Cong Chen,[a] Jianmeng Chen,[a] Zeyu Wang,[b] Jun Chen,*[b] Dzmitry Hrynshpan[c] and Tatsiana Savitskaya[c]

Nitrous oxide reductase (N_2OR) is the only known enzyme that can reduce the powerful greenhouse gas nitrous oxide (N_2O) to harmless nitrogen at the final step of bacterial denitrification. To alleviate the N_2O emission, emerging approaches aim at microbiome biotechnology. In this study, the genome sequence of facultative anaerobic bacteria *Pseudomonas citronellolis* WXP-4, which efficiently degrades N_2O, was obtained by *de novo* sequencing for the first time, and then, four key reductase structure coding genes related to complete denitrification were identified. The single structural encoding gene *nosZ* with a length of 1914 bp from strain WXP-4 was cloned in *Escherichia coli* BL21(DE3), and the N_2OR protein (76 kDa) was relatively highly efficiently expressed under the optimal inducing conditions of 1.0 mM IPTG, 5 h, and 30 °C. Denitrification experiment results confirmed that recombinant *E. coli* had strong denitrification ability and reduced 10 mg L^{-1} of N_2O to N_2 within 15 h under the optimal conditions of pH 7.0 and 40 °C, its corresponding N_2O reduction rate was almost 2.3 times that of *Alcaligenes denitrificans* strain TB, but only 80% of that of wild strain WXP-4, meaning that *nos* gene cluster auxiliary gene deletion decreased the activity of N_2OR. The 3D structure of N_2OR predicted on the basis of sequence homology found that electron transfer center CuA had only five amino acid ligands, and the S2 of the catalytically active center CuZ only bound one Cu_I atom. The unique 3D structure was different from previous reports and may be closely related to the strong N_2O reduction ability of strain WXP-4 and recombinant *E. coli*. The findings show a potential application of recombinant *E. coli* in alleviating the greenhouse effect and provide a new perspective for researching the relationship between structure and function of N_2OR.

Received 13th December 2021
Accepted 8th January 2022

DOI: 10.1039/d1ra09008a

rsc.li/rsc-advances

Introduction

Nitrous oxide (N_2O) is an inert, odorless and non-toxic gas that in particular acts as a powerful greenhouse gas and a significant depleter of ozone. Its global warming potential is more than 300 times that of carbon dioxide (CO_2).[1,2] N_2O is widely emitted due to fuel combustion, nitrogenous fertilizer utilization, and wastewater treatment, and can exist stably in the atmosphere for more than 100 years and its atmospheric concentration level is growing steadily at a rate of 0.2–0.3% per year.[3–5] So, the development of N_2O control technology is becoming increasingly important.

Biodegradation has attracted much attention due to its advantages, such as mild conditions, low cost, and no secondary pollution.[6,7] More than two-thirds of the global N_2O emissions originate from the soil ecosphere and hydrosphere, and can be reduced to harmless nitrogen gas (N_2) at the final step of the microbial denitrification pathway.[8–10] Nitrous oxide reductase (N_2OR) is the only enzyme that performs the biological denitrification process.[11,12] Thus, the efficient utilization of N_2OR is essential to the effective control of N_2O emission through biological methods.

N_2OR is a periplasmic multi-copper enzyme and a head-to-tail homodimer. Each monomer includes two domains: an electron transfer binuclear CuA center at C-terminal and a catalytic tetranuclear CuZ center at N-terminal.[13,14] Generally, CuA is liganded by six amino acid residues comprising one methionine, one tryptophan, two cysteines and two histidines; CuZ is coordinated by seven histidines.[15,16] On the base of the 3D structure of N_2OR, the consensus view of N_2O catalytic reduction mechanism is that N_2O binds to the catalytically active site of CuZ, then the electron is transferred from CuA to convert N_2O into N_2.

[a]*College of Environment, Zhejiang University of Technology, Hangzhou, 310014, China*
[b]*Key Laboratory of Pollution Exposure and Health Intervention of Zhejiang Province, Interdisciplinary Research Academy, Zhejiang Shuren University, Hangzhou, 310015, China. E-mail: bec@zjut.edu.cn; Tel: +86-571-88285209*
[c]*Research Institute of Physical and Chemical Problems, Belarusian State University, Minsk, 220030, Belarus*

† Electronic supplementary information (ESI) available. See DOI: 10.1039/d1ra09008a

N_2OR is encoded by the *nos* gene cluster (*nos*RZDFYL), in which *nos*Z gene is the structural gene.[17] In previous studies, the *nos*Z gene from various microbial groups has been successfully cloned and expressed in different hosts. Wan *et al.* reported that the transfer of *nos*Z gene into tobacco plants resulted in higher N_2OR activity and decreased N_2O release capacity.[18] Jones *et al.* found that when there were two copies of *nos*Z in *bacillus* cells, almost no N_2O was produced.[19] These results indicate that recombinant N_2OR plays an important role in reducing N_2O emissions. However, there are few systematic studies on the cloning and heterologous expression of *nos*Z gene, and its utilization needs to be further excavated.

Recently, a novel facultative anaerobic denitrifying bacteria showing high efficiency N_2O degradation, namely, *P. citronellolis* WXP-4, was isolated from the Qige sewage treatment plant (Hangzhou, China).[20] Its reduction efficiency is 100% at an initial N_2O concentration of 50 mg L^{-1} within 2 d (ESI Fig. S1†). Thus, it was intended to deeply understand *P. citronellolis* WXP-4. The aims of this study are as follows: (1) sequence the whole-genome of strain WXP-4 and identify the key denitrification genes; (2) clone the *nos*Z gene from strain WXP-4 in *E. coli* and investigate the N_2O removal performance of recombinant *E. coli*; (3) preliminarily explore the relation between the structure and function of N_2OR.

Materials and methods

Materials

P. citronellolis WXP-4 (CCTCC NO. M2018526) was isolated from the wastewater of Qige Sewage Treatment Plant (Hangzhou, China). *E. coli* BL21(DE3), plasmids pGEM-T and pET28a were purchased from TaKaRa Biotechnology Co., Ltd. PCR primer was purchased from Sangon Biotech (Shanghai, China). *Eco*R I and *Xho* I were purchased from Aoqian Biotech Co., Ltd (Hangzhou, China).

P. citronellolis WXP-4 and *E. coli* were grown in a sealed shake flask with LB medium comprising the following (per liter): NaCl (10.0 g), yeast extract (5.0 g), and peptone (10.0 g). The internal space of the sealed shake flask was guaranteed to be completely anaerobic by continuous rinsing with argon gas for 20 min through a sterile thin tube, which was inserted into the bottom of the culture medium. The medium used for N_2O degradation performance test was inorganic salt medium without nitrogen source as follows (per liter): sodium succinate (2.36 g), KH_2PO_4 (1.5 g), $Na_2HPO_4 \cdot 12H_2O$ (7.715 g), $MgSO_4 \cdot 7H_2O$ (0.1 g), agar (20.0 g), and trace element solution (2 mL). The trace element solution comprised the following (per liter): EDTA (5.0 g), $FeSO_4 \cdot 7H_2O$ (0.5 g), $ZnSO_4$ (0.43 g), $CuSO_4 \cdot 5H_2O$ (0.25 g), $CaCl_2$ (5.5 g), $CoCl_2 \cdot 6H_2O$ (0.24 g), $MnCl_2 \cdot 4H_2O$ (0.99 g), and H_3BO_4 (0.014 g). The rotation speed of the sealed shake flask was 160 rpm, the initial pH value of LB medium was set at 7.0, and the initial pH value of the inorganic salt medium without nitrogen source was the natural pH (~7.5).

The GenBank accession number for the genome sequence of strain *P. citronellolis* WXP-4 was CP034688 (these data were to be held confidential until: Dec 24, 2022).

De novo sequencing and coding genes prediction of *P. citronellolis* WXP-4

The genomic DNA of *P. citronellolis* WXP-4 was extracted by Gentra Puregene Yeast/Bact. Kit (Qiagen, Valencia, CA), and the nanopore library was constructed by using a nanopore sequencing kit. Afterward, second-generation sequencing was conducted by using Illumina high-throughput sequencer, and the third-generation real-time sequencing (single molecule sequencing) was conducted by using GridION X5 sequencer. The genome was assembled by the Unicycler (v0.4.5) software. The genome circle graph of *P. citronellolis* WXP-4 was drawn by using the online software Circos (v0.69) (http://www.circos.ca/software/download/circos/).

The genome annotation was performed by using the National Center for Biotechnology Information (NCBI) Prokaryotic Genome Annotation Pipeline (PGAP) system. The open reading frame (ORF) prediction was performed by using Prodigal gene-finding software v2.6.3.[21] Coding gene's function annotation was aligned with the databases of non-redundant protein (Nr), Kyoto Encyclopedia of Genes and Genomes (KEGG), and Clusters of Orthologous Groups (COG) by BLAST. Metabolic pathways were annotated by KEGG. The proteins encoded by genes were classified *via* phylogenetic classification by using COG. The composition, structure and location information of denitrification gene clusters in *P. citronellolis* WXP-4 were analyzed according to the annotation results. The gene structure map was drawn by using the SVG method.

TA cloning of *nos*Z gene

The genomic DNA of *P. citronellolis* WXP-4 was used as a DNA template for PCR. PCR was performed in a Mastercycler gradient (Bio-Rad, USA) by using the specific primers designed according to the *nos*Z gene sequence from strain WXP-4, as follows: *nos*Z-F (5′-GAATTCATGAACGAGAAGAAACACCCGCAGCCCGAAGACG-3′) and *nos*Z-R (5′-CTCGAGGGCCTTTTCCACCAGCATGCGGCCGACCATTTCC-3′). The PCR reaction system and reaction cycles refer to the method of Chen *et al.*[22] The PCR reaction system (50 μL) consisted of 25 μL of 2×Phanta Max Buffer, 1 μL of dNTPs Mix (10 μM), 2 μL of *nos*Z-F (10 μM), 2 μL of *nos*Z-R (10 μM), 1 μL of Phanta polymerase, 2 μL of template DNA, and 17 μL of double distilled water. The mixture was pre-denatured at 95 °C for 3 min. Then, it was denaturation at 95 °C for 0.5 min, annealed at 55 °C for 0.5 min, and extended at 72 °C for 1.5 min for a total of 33 cycles. Finally, extension was performed at 72 °C for 5 min. The PCR products obtained by SanPrep Rapid Gel DNA Recovery kit were added through "A" tail treatment using flat terminal DNA Fragment Plus "A" kit. Then, they were purified by SanPrep PCR and DNA Fragment Purification kit and ligated into pGEM-T plasmid to form a TA clone at 4 °C overnight. The TA clone was transformed into *E. coli* DH5α and conformed by colony PCR and restriction enzyme digestion. The positive colony plasmid was extracted by using the SanPrep Rapid Plasmid Extraction kit and sent to Youkang Biotech Co., Ltd (Hangzhou, China) for sequencing.

Bioinformatics analysis of *nosZ* gene and N_2OR protein

The sequence similarity of *nosZ* gene in *P. citronellolis* WXP-4 was compared with that of other strains by BLAST homology comparison on NCBI. The neighbor joining method in Mega software (v7.0.26) was used to construct the phylogenetic tree. DNAMAN software was used to analyze the length, base composition, and distribution of *nosZ* gene. The amino acid sequence was translated by gene transcription. The physical and chemical properties of N_2OR protein were analyzed by using the ProtParam online website (https://web.expasy.org/protparam/). The basic secondary structure of the protein was analyzed by the predict protein online website (https://www.predictprotein.org/). The Swiss Model online website (https://swissmodel.expasy.org/) was used to predict the 3D structure of the N_2OR protein based on the amino acid sequence in the PDB database. A homology model was generated using the N_2OR (PDB ID: 3SBP) from *P. stutzeri* as the template, with which N_2OR of strain WXP-4 shared 82.18% sequence identify, and the N_2OR protein was edited by using Discovery Studio 4.5 software.

Constructure and expression of recombinant *E. coli* BL21(DE3)-pET28a-*nosZ*

The pGEM-T-*nosZ* and pET28a plasmids were respectively extracted from the positive clone colony and *E. coli*. Then, they were simultaneously digested with *EcoR* I and *Xho* I. After the detection of enzyme digestion products by using agarose electrophoresis, the released *nosZ* gene was ligated into the treated pET28a plasmid at 4 °C overnight to construct the gene expression vector pET28a-*nosZ*. The constructed expression vector pET28a-*nosZ* was transformed into *E. coli* BL21(DE3), which was confirmed by colony PCR and restriction enzyme digestion. The recombinant *E. coli* BL21(DE3)-pET28a-*nosZ* was obtained for expression.

The recombinant *E. coli* was incubated in LB liquid medium containing 50 μg mL^{-1} of kanamycin and then cultured at 37 °C and 160 rpm until the logarithmic growth period. It was induced by IPTG at a final concentration of 1 mM for 5 h at 30 °C and 160 rpm. The total protein of all bacteria was extracted by ultrasonic method (power 400 watts, working for 3 s, intermittently for 2 s, and breaking 99 times) and purified by using His-tagged Protein Purification Kit (soluble protein, ESI S1.1†). SDS-PAGE (ESI S1.2†) was used to determine whether the recombinant N_2OR protein was expressed.

N_2O reduction performance and its influencing factors of recombinant *E. coli*

The recombinant *E. coli* was cultured and induced under the conditions mentioned above, three repeated experiments were set for each bacterial solution. The bacterial cells were harvested by centrifugation at 4 °C and 10 000 rpm for 5 min. Then, they were washed twice with 50 mL inorganic salt liquid medium without nitrogen source and transferred to the new 50 mL inorganic salt medium. Pure N_2O gas was injected into the headspace of a sealed shake flask with Agilent gas-tight syringe. The final concentrations of N_2O inside the shake flask reached 10, 20, 30, 40, and 50 mg L^{-1}. The concentrations of the remaining N_2O were measured regularly within 5 d to determine the N_2O degradation rate. The effects of factors, such as temperature (30 °C, 35 °C, 40 °C, 45 °C, and 50 °C) and pH (5.0, 6.0, 7.0, 8.0, and 9.0) on the degradation of 10 mg L^{-1} N_2O by recombinant *E. coli* were investigated. The remaining concentrations of N_2O were measured regularly in the shake flask by gas chromatography (Agilent 6890 N, USA).

The recombinant *E. coli* and *P. citronellolis* WXP-4 were cultured at respectively optimal conditions, then performed as mentioned above and three repeated experiments were set for each bacterial solution. The initial concentration of N_2O in the sealed flask was 10 mg L^{-1}. The remaining concentration of N_2O was measured regularly in the shake flask by Agilent gas chromatography (Agilent 6890 N, USA).

Analysis methods

Gas samples (250 μL) were regularly collected from the upper space of the shaker by GC-specific pointed gas-tight syringe and detected according to the previous method with slight modification.[23] N_2O was determined using an Agilent 6890 N GC equipped with an electron capture detector and a column (30 m × 0.32 mm × 0.25 μm) packed with HP-5. The temperatures of the column, injector, and detector were 40 °C, 100 °C, and 300 °C, respectively. The carrier gas was N_2 and flowed at a rate of 20 mL min^{-1}. All experiments were performed in triplicate. Data were presented as mean ± standard error and calculated by using the SPSS 13.0 software.

Results and discussion

Genome sequence and functional genes annotation of *P. citronellolis* WXP-4

The genomic DNA of *P. citronellolis* WXP-4 was sequenced by Illumina HiSeq. The sequencing clean data showed that the total genome length of strain WXP-4 was 6672752 bp, and the GC content was 67.40%. Then, the GC skew was calculated, which is the relative content of GC and is a useful tool for marking the start and end points of circular chromosomes. NCBI online database predicted that the genome contained 5757 coding sequences (CDS). Through sequence comparison with the Rfam database, 5756 mRNA, 15 rRNA, 66 tRNA, and 4 ncRNA were found in the genome (Fig. 1a).

The coding genes in WXP-4 genome were annotated by Nr, COG, and KEGG databases. Nr is the official protein sequence database of NCBI and typically used for species classification.[24] The number of annotated proteins was 5740, which accounted for 99.72% of the total protein number, and 99% of the CDS coding proteins were annotated as *Pseudomonas* sp. proteins by the database. The statistical results of genome COG showed that the strain WXP-4 contained 24 of 25 categories, and the number of genes responsible for amino acid transportation and metabolism ranked second (Fig. 1b). The metabolic pathways of gene products and compounds in cells and the functions of these gene products were systematically analyzed by KEGG. As

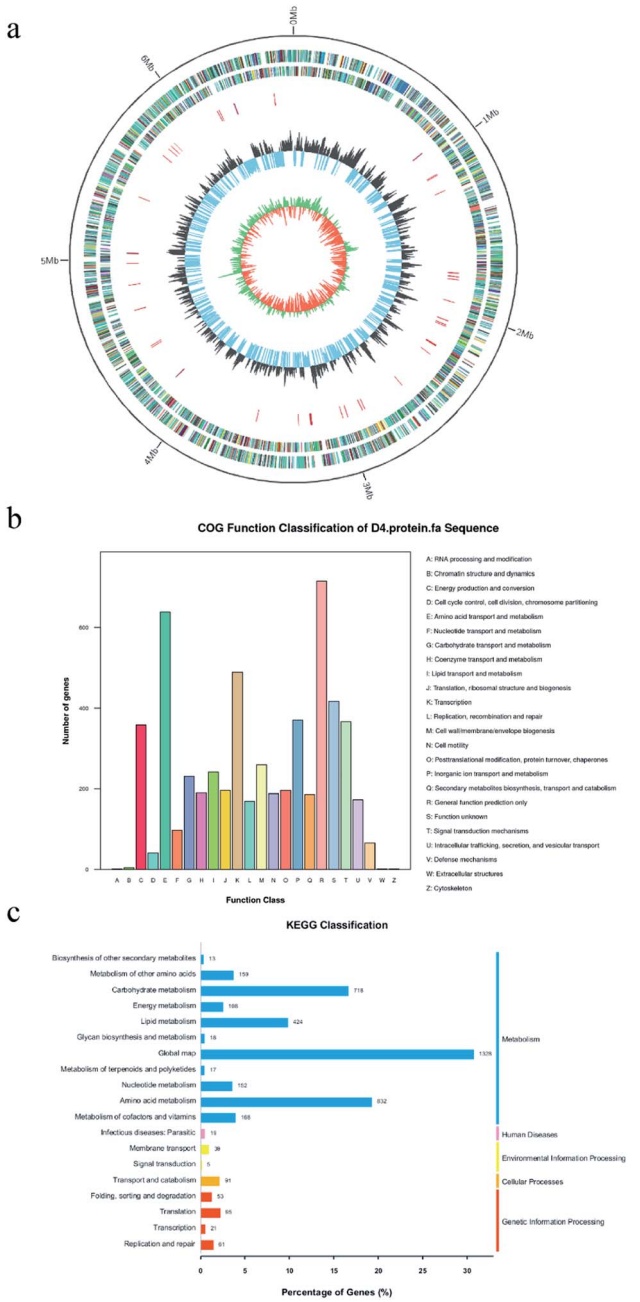

Fig. 1 (a) Genome circle of *P. citronellolis* WXP-4. In the above figure, there are six circles, from the inside to the outside: the first circle shows GC skew, the green part shows GC skew as a positive part, the orange part shows GC skew as a negative part; the second circle shows GC content; the third circle shows rRNA and tRNA annotation information, in which purple shows rRNA information and red shows tRNA information; the fourth and fifth circles show CDS annotation information, which is represented by different colors. The COG annotation classification of CDS is different, the fourth circle is that CDS is in the negative chain, the fifth circle is that CDS is in the positive chain; the outer circle shows the total genome size. (b) COG annotation classification chart. (c) KEGG annotation classification chart.

shown in Fig. 1c, 3952 genes in the genome were involved in the metabolism of bacteria, accounting for 91.14% of the total KEGG annotation genes. Among these, 718 genes were involved in carbohydrate metabolism; 852 genes were involved in amino acid metabolism; 135 genes were involved in environmental information processing and cellular processes; and 249 genes were involved in the three pathways of the biological system, human disease, and genetic information processing.

Identification of denitrification genes in *P. citronellolis* WXP-4

The complete denitrification process includes four reductases, namely, nitrate reductase (Nar), nitrite reductase (Nir), nitric oxide reductase (NOR), and N_2OR, which were coded by specific genes.[25] A total of 25 denitrification genes were found in strain WXP-4. Part of these genes constituted the *nar* and *nos* denitrification gene clusters, whereas the other *nir* and *nor* genes were not clustered separately. The *nar*, *nir*, and *nor* genes were relatively close to one another on the chromosome. The denitrification gene clusters were arranged in an orderly and relatively compact manner.

According to their different locations in the cell, denitrifying bacteria usually express two kinds of Nar, namely, membrane-bound and periplasmic-bound nitrate reductase; their coding genes were usually *nar* and *nap*, respectively.[26] In *P. citronellolis* WXP-4, only *nar* existed and was present in the form of a gene cluster. The *nar* gene cluster with a total length of 18.02 kb was located on the antisense chain of the genome and encoded 12 ORFs, namely, *nar*L, *nar*Q, *nar*K-2, *nar*K-1, *nar*G, *nar*H, *nar*J, *nar*I, *nar*G, *nar*H, *nar*J, and *nar*I, in order (Fig. 2a). Twelve regularly arranged genes were transcribed in the same direction on the chromosome, and no gap was found in the coding

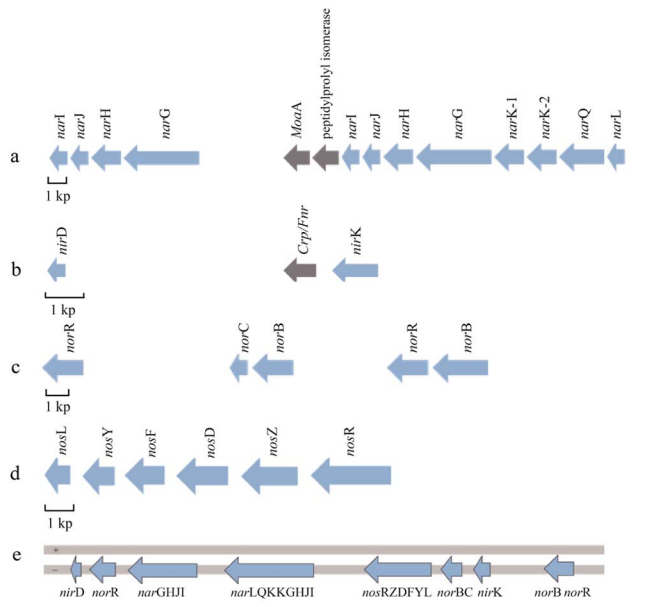

Fig. 2 Schematic diagram of denitrification gene clusters arrangement in *P. citronellolis* WXP-4. (a) *nar* gene cluster, (b) *nir* gene cluster, (c) *nor* gene cluster, (d) *nos* gene cluster. (e) Location map of the denitrifying genes on the genome of strain WXP-4. The direction of the arrow indicates the direction of transcription. The blue arrow represents the denitrification gene, while gray arrow represents other genes. + indicates the genomic sense strand, − indicates the genomic antisense strand.

region. Among these genes, *nar*GHI was the structural gene of Nar, whereas the others were the auxiliary genes of the enzyme. The largest ORF gene was *nar*G with a length of 3780 bp; it encoded the α subunit of Nar. The *nar*H and *nar*I encoded the β and γ subunits of nitrate reductase, respectively. The *nar*J encoded the Mo cofactor assembly chaperone of Nar.[27]

Nir catalyzes the reduction of nitrite to nitric oxide, which is the most important rate-limiting step in the denitrification process. Nir is generally divided into cytochrome cd1-type Nir and Cu-type Nir, which are encoded by *nir*S and *nir*K genes, respectively.[28,29] However, these two enzymes generally do not coexist in one bacterium. Only one copy of the *nir*K gene was found in the strain WXP-4, whereas other conventional *nir* genes did not exist near the upstream and downstream, and *nir*D genes were found far upstream (Fig. 2b); this might be the evolutionary difference from other bacteria. Possibly, some *nir* genes have not yet been identified. A search for *nir*-related proteins in the *P. citronellolis* WXP-4 genome needs to be performed in the future. All the key genes involved in the nitrite reduction process and their functions need to be identified.

NOR reduces NO to N_2O, which can be divided into two types, namely, cNOR and qNOR. cNOR is a heterodimer oligomerase that is encoded by *nor*B and *nor*C, some regulatory genes may be present. qNOR is a monomer enzyme encoded by a single gene, either *nor*B or *nor*Z.[30,31] Strain WXP-4 only contains cNOR. Two copies of *nor*B and *nor*R were found in the genome of strain WXP-4, but they were far away. One of the *nor*B genes (1422 bp) was downstream of *nor*C (441 bp). The other *nor*B gene (2279 bp) was downstream of *nor*R (1565 bp), which functions in NOR transcriptional regulation (Fig. 2c).

Compared with other denitrifying gene clusters, the *nos* gene clusters were very conservative. They were all arranged in the genome with a sequence of *nos*RZDFYL.[32] In *P. citronellolis* WXP-4, the coding genes of N_2OR formed the *nos* gene cluster, which was transcribed in the same direction, had a relatively compact arrangement, and had no other genes inside. In addition, the total length of the *nos* gene cluster was 7554 bp and included six ORFs in the following order: *nos*R, *nos*Z, *nos*D, *nos*F, *nos*Y, and *nos*L (Fig. 2d). Among them, the longest gene was *nos*R gene (2115 bp), which encodes an integral membrane protein required for electron delivery and function. The structural *nos*Z gene with a length of 1914 bp encodes the N_2OR protein. The *nos*DFY genes encode an ABC transporter (NosFY) and a periplasmic interacting protein, NosD, which is presumably required for shuttling a sulfur species into the periplasm for CuZ assembly. The *nos*L encodes a membrane anchored copper molecular chaperone.[33,34]

According to the whole genome sequence, four key reductase structure coding genes were involved in the denitrification of WXP-4, as follows: *nar*GHI, *nir*K, *nor*CB, and *nos*Z, demonstrating that *P. citronellolis* WXP-4 was a complete denitrifying bacterium. These results further confirmed the research results of Wang *et al.*[20] According to the position of these four structure genes in the genome, the gene map was drawn and shown in Fig. 2e. The *nos*, *nor*, *nir*, and *nar* genes were arranged on the genome chain in order.

TA cloning and basic sequence of *nos*Z gene

The *nos*Z gene encoding N_2OR in strain WXP-4 was amplified by PCR and obtained by TA cloning. The results of the agarose gel electrophoresis of the *nos*Z gene PCR products demonstrated that the target DNA band was clear (ESI Fig. S2†), indicating the reaction conditions are appropriate. Generally, the number of PCR cycles will be selected between 30–35, which depends on the concentration of template DNA and other substances in the reaction system. Too few cycles will result in insufficient amplification of target DNA, and the more cycles will produce the more non-specific products. The analysis results from DNAMAN software showed that the total length of *nos*Z gene was 1914 bp, and the ATCG base contained 390, 266, 583, 675, which accounted for 20.4%, 13.9%, 30.5%, and 35.3% of the total base number respectively. The BLAST homology comparison results revealed that the nucleotide sequence of *nos*Z gene was like that of the encoding N_2OR protein in *P. aeruginos*a HS9. The phylogenetic tree showed that the confidence of *nos*Z sequence homology between strain WXP-4 and *P. aeruginosa* was 100 (Fig. 3).

The analysis of the *nos*Z sequence found the presence of 101 restriction endonucleases in the sequence, which could be digested by 49 restriction enzymes. However, the restriction

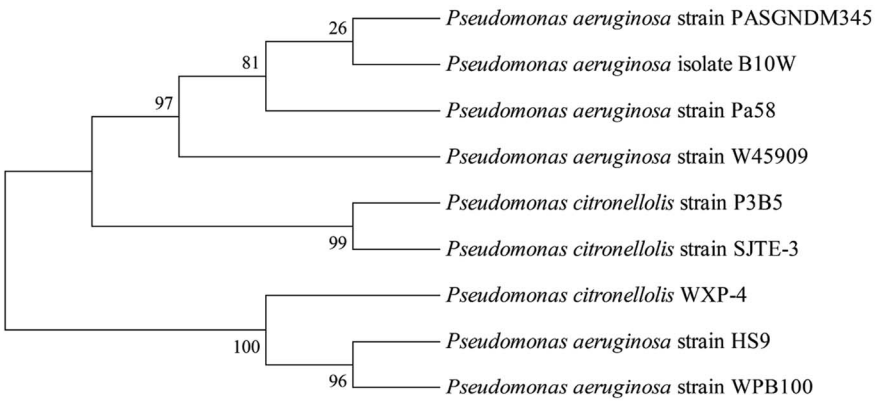

Fig. 3 Phylogenetic tree of *nos*Z gene in *P. citronellolis* WXP-4. The phylogenetic tree is constructed by using the NJ method. The bootstrap value is set to 1000. Scale bars represent the estimated number of nucleotide substitutions per site.

endonucleases of *Eco*R I and *Xho* I were absent (ESI Fig. S3†). The sequence could be inserted into other vectors *via Eco*R I and *Xho* I double enzyme digestion without sequence self-cutting. The restriction endonuclease site map and electrophoretic simulation of single enzyme digestion of *nos*Z gene with 49 restriction enzymes were shown in Fig. S3.†

Spatial structure of the N_2OR protein

The basic physical and chemical properties of N_2OR protein analyzed by ProtParam tool showed that the *nos*Z protein contained 20 kinds and 637 amino acids, and the predicted molecular mass of the protein was 70.9 kDa. Like the N_2OR of *W. succinogenes* and *P. putida* HK_5, the predicted 3D structure of N_2OR protein in *P. citronellolis* WXP-4 was a head-to-tail homodimer and each monomer contains CuZ center and CuA center.[35,36] The distance between the CuA center from one monomer and the CuZ center from the other monomer was approximately 11.7 Å, and the distance between two copper centers in one monomer was about 41 Å, which were too far away for effective electron transfer (Fig. 4a).[3] In addition, the CuA center comprising two copper atoms was only coordinated by five conserved amino acid residues (C617, C621, H625, T619, and M628), CuZ center consisting of four copper atoms and two sulfur atoms comprised seven conserved histidine residues (H325, H177, H381, H432, H493, H128, and H129), but the S2 atom only bound one Cu_I atom (Fig. 4b). These results were different from *P. stutzeri* and *P. nautica*, in which the CuA had six amino acid ligands and the S2 atom both bound Cu_I and Cu_{IV} atoms.[15,16]

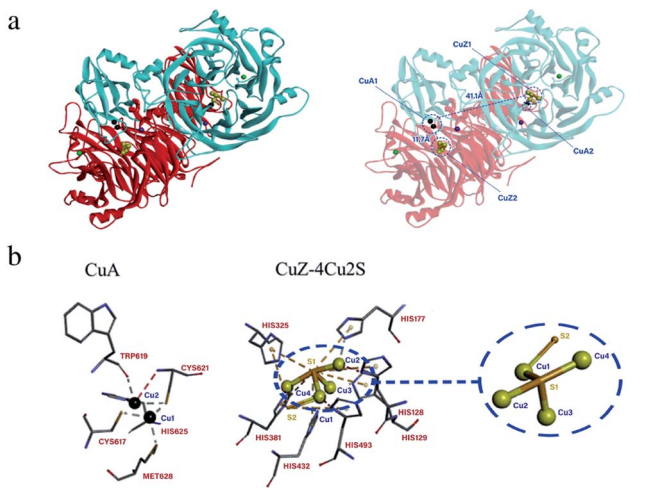

Fig. 4 The structure of N_2OR from *P. citronellolis* WXP-4 edited by using Discovery Studio 4.5 software. (a) The structure of N_2OR and the distance between copper atoms. (b) Central amino acid coordination of CuA and CuZ. The dimer is colored according to subunit, with one monomer colored blue and the other red. The CuA and CuZ centers are colored in black and gold, respectively. The copper atoms in the CuA and CuZ centers are numbered 1 and 2 or 1, 2, 3 and 4.

CuA site is a mixed-valent center that leads to a low reorganization energy, making CuA an efficient electron transfer agent.[37,38] Among the ligands of CuA from *P. stutzeri* N_2OR, His583 plays a role in electron gating to CuA. But in the CuA of *P. citronellolis* WXP-4 N_2OR, no similar His583 ligand was found, which may be due to the unbound conformation of H583 or is derived from a different bacterium.[39] In previous research, the more labile S2 was found to bridge ions Cu_I and Cu_{IV} in two monomers and prone to be replaced by a water ligand.[34] Therefore, the S2 atom only bound one Cu_I atom in *P. citronellolis* WXP-4, which seems to be more easily affected by other ligand than when the S2 atom binds two Cu atoms, meaning that N_2O may more easily bind to CuZ active sites.

N_2OR expression in recombinant *E. coli*

As shown in Fig. S4,† the growth adaptation period of recombinant *E. coli* was relatively short. It reached the logarithmic phase after 2 h of inoculation. After inoculation for 10 h, the recombinant *E. coli* reached a stable period, and OD_{600} no longer changed significantly. The enhanced expression of N_2OR was performed by inducer IPTG, which tightly related to inducer addition time. The addition of inducers in

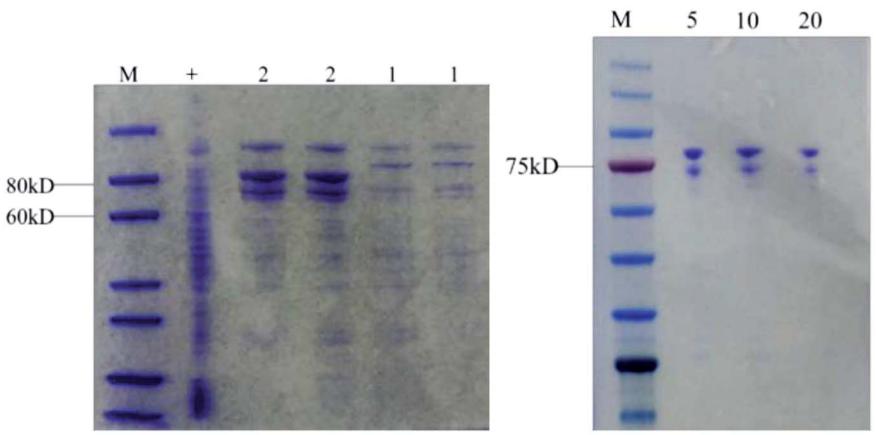

Fig. 5 SDS-PAGE electrophoresis analysis of N_2OR protein. M: protein marker; 1: not induced by IPTG; 2: induced by IPTG; +: positive control (wild bacteria); 5, 10 and 20: the purified N_2OR was diluted 5 times, 10 times and 20 times respectively.

the middle and early logarithmic stages of bacterial growth promoted gene expression and high protein concentrations.[10,40] The addition of the inducer during the lag phase makes bacterial growth difficult; its addition during the stabilization phase inhibits the expression of the target gene.[41] Generally, the optimal OD_{600} interval for gene induced expression should be in the range of 0.5–0.8. In this study, the OD_{600} was selected as 0.6, and the culture time was 2 h. The optimal induce conditions were 1.0 mM IPTG, 5 h, and 30 °C. After protein extraction, isolation, and purification, the expression of the *nos*Z gene was examined by SDS-PAGE gel electrophoresis, and the results were shown in Fig. 5.

The target band appeared at 76 kDa and was congruent with the SDS-PAGE gel electrophoresis results. The theoretical value of the molecular mass of the protein removed by *Eco*R I and *Xho* I was about 1.446 kDa. The expression of the remaining protein on pET28a was about 5.230 kDa. The target protein N_2OR was about 70.9 kDa. The molecular mass of the fusion protein was about 76.033 kDa. This finding demonstrated that N_2OR was successfully expressed in *E. coli* BL21(DE3)-pET28a-*nos*Z from one side. The band on the left panel became brighter when the recombinant *E. coli* was induced by IPTG, which indicated that IPTG promoted the expression of the target protein. Meanwhile, when the N_2OR was not diluted, more than five bands were observed on the electrophoresis graph. However, after dilution, the number of electrophoresis bands was significantly reduced, which was probably due to high protein concentration or protein purity.

The reduction performance of recombinant *E. coli* on N_2O

To verify the activity of N_2OR protein expressed by recombinant *E. coli* and the reduction performance of N_2O, the N_2O degradation amount in the N_2O reduction system with different initial concentrations (10, 20, 30, 40, and 50 mg L^{-1}) was determined. As shown in Fig. 6a, the N_2O degradation time increased with increasing initial concentration of N_2O. When the initial concentration was 10 mg L^{-1}, the effect of complete removal was achieved within 2 d. The results proved that the *nos*Z gene was transcribed in *E. coli* BL21(DE3) to activate the N_2OR protein.

The factors that affect the activity of N_2OR, such as pH and temperature, were investigated. When the pH value was 7.0 and 8.0, the reducing effect on N_2O was the most significant, reaching 100% and 98% of the relative activity percentage, respectively (Fig. 6b). The results coincided with the findings by Fujita and Dooley, which suggested that the neutral or slightly alkaline environment is conducive to the development of N_2OR activity.[42] Therefore, the optimum pH for N_2OR activity was 7 or 8. The amount of reduced N_2O reached the maximum value at 40 °C (Fig. 6c), whereas the activity of N_2OR decreased significantly at low and high temperatures. The results were the same as the findings of Ferretti *et al.*[43]

The N_2O reduction performances of recombinant *E. coli* and *P. citronellolis* WXP-4 were compared, as presented in Fig. 7. Under the optimal conditions of pH 7.0 and 40 °C, the recombinant *E. coli* could reduce 10 mg L^{-1} of N_2O to N_2 within

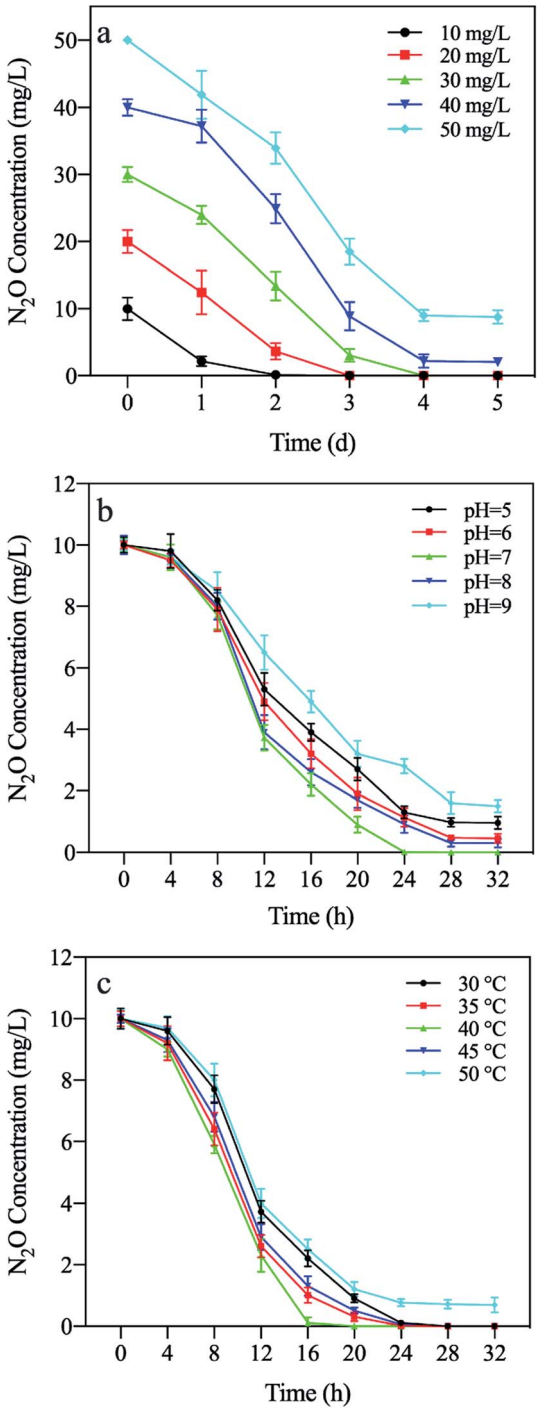

Fig. 6 Effect of different conditions on N_2O reduction of recombinant *E. coli*. (a) initial N_2O concentration. (b) pH. (c) temperature.

15 h, which corresponded to a reduction rate of 0.67 mg $(L\ h)^{-1}$ and was almost 2.3 times that of *Alcaligenes denitrificans* strain TB (0.29 mg $(L\ h)^{-1}$).[10] However, the reduction rate of recombinant *E. coli* was only 80% of that of wild strain WXP-4, and this result may be due to the deletion of one or several genes in the *nos*RDFYL gene, which encodes the auxiliary protein related to N_2OR activity or total enzymes quantity.[13,22]

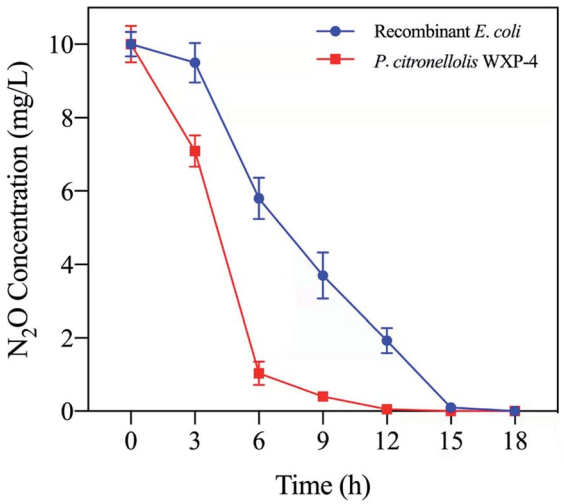

Fig. 7 Comparison of N_2O reduction performance between *P. citronellolis* WXP-4 and recombinant *E. coli*.

Fortunately, heterologous host *E. coli* maybe has a certain compensation mechanism which can partially compensate for the function of deletion gene, so that the recombinant *E. coli* can still have strong N_2O reduction properties, indicating *E. coli* is an ideal host for heterologous expression and a highly suitable tool to further investigate the mechanism of N_2O reduction.[34] Overall, both recombinant *E. coli* and wild strain WXP-4 have strong N_2O reduction ability, which may be closely related to the unique 3D structure of strain WXP-4 N_2OR (CuA had only five amino acid ligands and the S2 of CuZ only bound Cu_I atom), its related mechanism needs to be further studied.

Conclusions

In this work, the whole genome sequence of *P. citronellolis* WXP-4 was determined for the first time and four key reductase structure coding genes related to complete denitrification were identified. Then single structural coding gene *nos*Z was cloned and the recombinant *E. coli* BL21(DE3)-pET28a-*nosZ* was successfully constructed. It exhibited strong N_2O reduction ability and completely reduced 10 mg L^{-1} N_2O to N_2 within 15 h under optimal conditions (pH 7.0 and 40 °C), corresponding the N_2O reduction rate was almost 2.3 times that of *Alcaligenes denitrificans* strain TB, but only 80% of that of wild strain WXP-4. It was induced that *nos* gene cluster auxiliary gene deletion decreased the activity of N_2OR. The 3D structure of N_2OR was explored, and the predicted results showed that the electron transfer center CuA had only five amino acid ligands, and S2 of the 4Cu:2S structural catalytically active center CuZ only bound one Cu_I atom. The unique 3D structure was different from the results of previous studies and maybe closely related to the strong N_2O reduction ability. These findings provide a potential candidate for decreasing the greenhouse effect and a new perspective for studying the structure–activity relationship of N_2OR.

Author contributions

Liyong Hu: formal analysis, investigation, writing – review & editing, project administration. Xiaoping Wang: formal analysis, investigation, software, writing – original draft. Cong Chen: validation, data curation, writing – review & editing. Jianmeng Chen: resources, supervision. Zeyu Wang: validation, data curation. Jun Chen: methodology, conceptualization, funding acquisition, writing – review & editing, supervision. Dzmitry Hrynshpan: methodology. Tatsiana Savitskaya: methodology.

Conflicts of interest

There are no conflicts to declare.

Acknowledgements

This work was supported by the National Primary Research & Development Plan (2018YFE0120300), the National Natural Science Foundation of China (21777142, 22011530015), Zhejiang Provincial Department of Education Research Project (Natural Science), and Zhejiang Shuren University Basic Scientific Research Special Funds (2020XZ012).

References

1 E. M. Johnston, C. Carreira, S. Dell'Acqua, S. G. Dey, S. R. Pauleta, I. Moura and E. I. Solomon, *J. Am. Chem. Soc.*, 2017, **139**, 4462–4476.
2 J. M. Blum, Q. Su, Y. Ma, B. Valverde-Pérez, C. Domingo-Félez, M. M. Jensen and B. F. Smets, *Environ. Microbiol.*, 2018, **20**, 1623–1640.
3 D. Richardson, H. Felgate, N. Watmough, A. Thomson and E. Baggs, *Trends Biotechnol.*, 2009, **27**, 388–397.
4 J. W. Zou, Y. Y. Lu and Y. Huang, *Environ. Pollut.*, 2010, **158**, 631–635.
5 M. S. Zheng, N. Zhou, S. S. He, F. Chang, J. Zhong, S. Xu, Z. Wang and T. Liu, *J. Environ. Manage.*, 2021, **280**, 111657.
6 C. Kennes, E. R. Rene and M. C. Veiga, *J. Chem. Technol. Biotechnol.*, 2009, **84**, 1419–1436.
7 L. R. Bakken, L. Bergaust, B. Liu and Å. Frostegård, *Philos. Trans. R. Soc., B*, 2012, **367**, 1226–1234.
8 K. Lassey and M. Harvey, *Water Atmos.*, 2007, **2**, 10–11.
9 D. Fowler, M. Coyle, U. Skiba, M. A. Sutton, J. N. Cape, S. Reis, L. J. Sheppard, A. Jenkins, B. Grizzetti, J. N. Galloway, P. Vitousek, A. Leach, A. F. Bouwman, K. Butterbach-Bahl, F. Dentener, D. Stevenson, M. Amann and M. Voss, *Philos. Trans. R. Soc., B*, 2013, **368**, 20130112.
10 Y. Wang, Z. Y. Wang, Y. K. Duo, X. P. Wang, J. M. Chen and J. Chen, *Environ. Pollut.*, 2018, **239**, 43–52.
11 C. Carreira, S. R. Pauleta and I. Moura, *J. Inorg. Biochem.*, 2017, **177**, 423–434.
12 M. M. M. Kuypers, H. K. Marchant and B. Kartal, *Nat. Rev. Microbiol.*, 2018, **16**, 263–276.
13 S. R. Pauleta, S. Dell'Acqua and I. Moura, *Coord. Chem. Rev.*, 2013, **257**, 332–349.

14 E. M. Johnston, S. Dell'Acqua, S. Ramos, S. R. Pauleta, I. Moura and E. I. Solomon, *J. Am. Chem. Soc.*, 2014, **136**, 614–617.
15 A. Pomowski, W. Zumft, P. Kroneck and O. Einsle, *Nature*, 2011, **477**, 234–237.
16 E. M. Johnston, S. Dell'Acqua, S. R. Pauleta, I. Moura and E. I. Solomon, *Chem. Sci.*, 2015, **6**, 5670–5679.
17 L. Q. Yang, X. J. Zhang and X. T. Ju, *Sci. Rep.*, 2017, **7**, 43283.
18 S. Wan, T. Greenham, K. Goto, Y. Mottiar, A. M. Johnson, J. Staebler, M. Zaidi, Q. Shu and I. Altosaar, *Can. J. Plant Sci.*, 2014, **94**, 1013–1023.
19 C. M. Jones, A. Welsh, I. N. Throbäck, P. Dörsch, L. R. Bakken and S. Hallin, *FEMS Microbiol. Ecol.*, 2011, **76**, 541–552.
20 X. P. Wang, Y. K. Duo, J. J. He, J. C. Yao, H. F. Qian, D. Hrynsphan, S. Tatsiana and J. Chen, *Bioprocess Biosyst. Eng.*, 2020, **43**, 811–820.
21 D. Hyatt, G. L. Chen, P. F. LoCascio, M. L. Land, F. W. Larimer and L. J. Hauser, *BMC Bioinf.*, 2010, **11**, 119.
22 C. Chen, Y. Wang, H. Liu, Y. Chen, J. C. Yao, J. Chen, D. Hrynsphan and S. Tatsiana, *Chemosphere*, 2020, **253**, 126739.
23 Y. L. Lei, Y. Q. Wang, H. J. Liu, C. W. Xi and L. Y. Song, *Appl. Microbiol. Biotechnol.*, 2016, **100**, 4219–4229.
24 A. G. Kennedy, *J. Eval. Clin. Pract.*, 2017, **23**, 959–963.
25 W. G. Zumft, *Microbiol. Mol. Biol. Rev.*, 1997, **61**, 533–616.
26 L. Philippot, *Biochim. Biophys. Acta*, 2002, **1577**, 355–376.
27 J. M. Dow, S. Grahl, R. Ward, R. Evans, O. Byron, D. G. Norman, T. Palmer and F. Sargent, *FEBS J.*, 2014, **281**, 246–260.
28 S. Henry, D. Bru, B. Stres, S. Hallet and L. Philippot, *Appl. Environ. Microbiol.*, 2006, **72**, 5181–5189.
29 C. Sánchez and K. Minamisawa, *FEMS Microbiol. Lett.*, 2018, **365**, 1–7.
30 N. Gonska, D. Young, R. Yuki, T. Okamoto, T. Hisano, S. Antonyuk, S. S. Hasnain, K. Muramoto, Y. Shiro, T. Tosha and P. Adelroth, *Sci. Rep.*, 2018, **8**, 3637.
31 R. Yamagiwa, T. Kurahashi, M. Takeda, M. Adachi, H. Nakamura, H. Arai, Y. Shiro, H. Sawai and T. Tosha, *Biochim. Biophys. Acta, Bioenerg.*, 2018, **1859**, 333–341.
32 L. Philippot, P. Mirleau, S. Mazurier, S. Siblot, A. Hartmann, P. Lemanceau and J. C. Germon, *Biochim. Biophys. Acta*, 2001, **1571**, 436–440.
33 V. V. Kadnikov, A. V. Mardanov, O. A. Podosokorskaya, S. N. Gavrilov, I. V. Kublanov, A. V. Beletsky, E. A. Bonch-Osmolovskaya and N. V. Ravin, *PLoS One*, 2013, **8**, e53047.
34 L. Zhang, A. Wüsta, B. Prassera, C. Müllera and O. Einslea, *PNAS*, 2019, **116**, 12822–12827.
35 Z. Chen, K. Matsushita, T. Yamashita, T. Fujii, H. Toyama, O. Adachi, H. D. Bellamy and F. S. Mathews, *Structure*, 2002, **10**, 837–849.
36 S. Dell'Acqua, I. Moura, J. J. G. Moura and S. R. Pauleta, *J. Biol. Inorg Chem.*, 2011, **16**, 1241–1254.
37 O. Farver, Y. Lu, M. C. Ang and I. Pecht, *Proc. Natl. Acad. Sci. U. S. A.*, 1999, **96**, 899–902.
38 P. Kroneck, *J. Biol. Inorg Chem.*, 2018, **23**, 27–39.
39 L. Zhang, E. Bill, P. Kroneck and O. Einsle, *J. Am. Chem. Soc.*, 2021, **143**, 830–838.
40 X. Y. Ou, F. Peng, X. L. Wu, P. Xu, M. H. Zong and W. Y. Lou, *Biochem. Eng. J.*, 2020, **158**, 107573.
41 N. Van Noi and Y. C. Chung, *Biotechnol. Biotechnol. Equip.*, 2017, **31**, 619–629.
42 K. Fujita and D. M. Dooley, *Inorg. Chem.*, 2007, **46**, 613–615.
43 S. Ferretti, J. G. Grossmann, S. S. Hasnain, R. R. Eady and B. E. Smith, *Eur. J. Biochem.*, 1999, **259**, 651–659.